Spectral, electrochemical, and photophysical studies of a magnesium porphyrin–fullerene dyad

ARTICLE *in* PHYSICAL CHEMISTRY CHEMICAL PHYSICS · OCTOBER 2005

Impact Factor: 4.49 · DOI: 10.1039/b507673k · Source: PubMed

RESEARCH PAPER

PCCP
www.rsc.org/pccp

Spectral, electrochemical, and photophysical studies of a magnesium porphyrin–fullerene dyad†

Mohamed E. El-Khouly,[a] Yasuyuki Araki,[a] Osamu Ito,*[a] Suresh Gadde,[b] Amy L. McCarty,[b] Paul A. Karr,[b] Melvin E. Zandler[b] and Francis D'Souza*[b]

[a] *Institute of Multidisciplinary Research for Advanced Materials, Tohoku University, Katahira, Sendai 980-8577, Japan. E-mail: ito@tagen.tohoku.ac.jp; Fax: +81-22-217-5610*

[b] *Department of Chemistry, Wichita State University, 1845 Fairmount, Wichita, KS 67260-0051, USA. E-mail: Francis.DSouza@wichita.edu; Fax: +316-978-3431*

Received 31st May 2005, Accepted 15th July 2005
First published as an Advance Article on the web 29th July 2005

A covalently linked magnesium porphyrin–fullerene (MgP*o*–C_{60}) dyad was synthesized and its spectral, electrochemical, molecular orbital, and photophysical properties were investigated and the results were compared to the earlier reported zinc porphyrin–fullerene (ZnP*o*–C_{60}) dyad. The *ab initio* B3LYP/3-21G(*) computed geometry and electronic structure of the dyad predicted that the HOMO and LUMO are mainly localized on the MgP and C_{60} units, respectively. In *o*-dichlorobenzene containing 0.1 M $(n\text{-Bu})_4NClO_4$, the synthesized dyad exhibited six one-electron reversible redox reactions within the potential window of the solvent. The oxidation and reduction potentials of the MgP and C_{60} units indicate stabilization of the charge-separated state. The emission, monitored by both steady-state and time-resolved techniques, revealed efficient quenching of the singlet excited state of the MgP and C_{60} units. The quenching pathway of the singlet excited MgP moiety involved energy transfer to the appended C_{60} moiety, generating the singlet excited C_{60} moiety, from which subsequent charge-separation occurred. The charge recombination rates, k_{CR}, evaluated from nanosecond transient absorption studies, were found to be 2–3 orders of magnitude smaller than the charge separation rate, k_{CS}. In *o*-dichlorobenzene, the lifetime of the radical ion-pair, MgP$o^{\bullet+}$–$C_{60}^{\bullet-}$, was found to be 520 ns which is longer than that of ZnP$o^{\bullet+}$–$C_{60}^{\bullet-}$ indicating better charge stabilization in MgP*o*–C_{60}. Additional prolongation of the lifetime of MgP$o^{\bullet+}$–$C_{60}^{\bullet-}$ was achieved by coordinating nitrogenous axial ligands. The solvent effect in controlling the rates of forward and reverse electron transfer is also investigated.

Introduction

Studies on photoinduced energy- and electron transfer in molecular and supramolecular systems have witnessed a rapid growth in the past decade.[1–9] These studies were aimed to address mechanistic details of light induced processes in chemistry and biology, and also, to develop molecular optoelectronic devices.[10] Fullerenes, as 3-D electron acceptors,[11] and porphyrins, often addressed as the pigment of life, as electron donors[12] have been utilized in the construction of such dyads owing to their well-understood electrochemical, optical, and photochemical properties.[9,13–14] The reorganization energy in electron transfer reactions for fullerenes was found to be small due to their unique structure and symmetry.[15] As a consequence, fullerenes (C_{60} and C_{70}) in donor–acceptor dyads accelerate forward electron transfer (k_{CS}) and slow down backward electron transfer (k_{CR}) resulting in the formation of long-lived charge-separated states. That is, the forward electron transfer occurs in the normal region of the Marcus curve[1] while the backward electron transfer occurs in the inverted region of the Marcus curve.[15] Several porphyrin–fullerene dyads, triads, tetrads, *etc.* have been designed and studied to probe the effect of molecular topology, and distance and orientation effects on the charge stabilization process.[8,14,16–18]

Several factors are known to affect k_{CS} and k_{CR} in molecular and supramolecular donor–acceptor dyads, *viz.*, the nature and rigidity of the connecting bonds, spatial organization, distance between the donor and acceptor entities, solvent media, temperature, *etc.*[1–9] Additionally, another factor that could be changed in porphyrin–acceptor type dyads is the central metal ion in the porphyrin cavity. However, only a handful of metalloporphyrins are fluorescent and some of them are known to be unstable, which limits their utilization in the study of energy- and electron transfer from the photo-excited singlet states.[12] As a result, the majority of the covalently linked porphyrin–fullerene dyads studied to date have utilized either free-base porphyrin or zinc porphyrin as donors.

Magnesium porphyrins are fluorescent compounds bearing a diamagnetic metal ion of ionic radius of *ca.* 0.72 Å[19] in the porphyrin cavity. Although both zinc and magnesium porphyrins display quite similar optical absorption and emission properties, magnesium porphyrins exhibit higher fluorescence quantum yields and longer excited state lifetimes (8–10 ns) compared to zinc porphyrins (2–2.5 ns).[20] Importantly, magnesium porphyrins are easier to oxidize by over 250 mV due to the less electronegative magnesium.[21] This property in turn increases the exothermicity of electron transfer reactions in magnesium porphyrin bearing donor–acceptor dyads.[22]

A few covalently linked magnesium porphyrin–acceptor type dyads have been synthesized and photoinduced energy- and electron transfer in these systems have been reported.[22] A few studies have also utilized magnesium porphyrins to build optoelectronic devices.[10,19*b*,23,24] Recently, we utilized magnesium porphyrin to build a supramolecular magnesium porphyrin–fullerene dyad by axial coordination using an imidazole

† Electronic supplementary information (ESI) available: Visible spectral changes observed for MgP*o*–C_{60} on increasing addition of pyridine in toluene; absorption spectra of MgP*o*–C_{60} in toluene, anisole, benzonitrile and argon saturated solution; fluorescence decay profiles (Fig. S1–S8). See http://dx.doi.org/10.1039/b507673k

DOI: 10.1039/b507673k

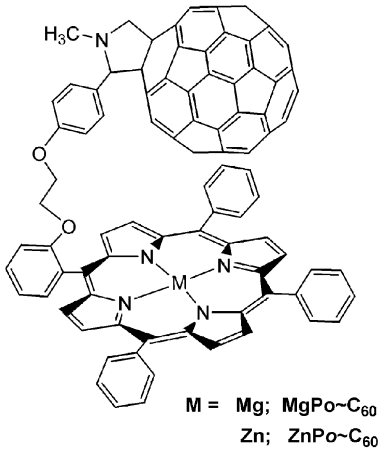

Scheme 1 Structures of the investigated porphyrin–fullerene dyads.

appended fullerene.[25] In the present study, we have successfully synthesized a covalently linked magnesium porphyrin–fullerene dyad (Scheme 1), and photoinduced electron/energy transfer has been systematically investigated. The structure of the MgP*o*–C_{60} dyad investigated here is similar to the previously studied zinc porphyrin–fullerene dyad[26a] (Scheme 1). Hence, it has been possible to compare the results with respect to the effect of the central metal ion of the porphyrin cavity on the photoinduced charge separation and charge recombination in these dyads. The photochemical events were also probed in solvents of different polarity and axial binding ability to probe their effects on charge stabilization.

Results and discussion

Syntheses

The syntheses of MgP*o*–C_{60} and the reference compound, *meso*-tetraphenylporphyrinato-magnesium(II), MgTPP, are given in the Experimental section. The structural integrity of all of the compounds was deduced from ^{1}H NMR, ESI mass in a CH_2Cl_2 matrix, optical absorption and emission, and electrochemical methods.

UV-visible spectral studies

Fig. 1a shows the optical absorption spectra of MgP*o*–C_{60} in *o*-dichlorobenzene. The spectral features in the visible range are characteristic of magnesium tetraphenylporphyrin, MgTPP.[22,23] An absorption band in the UV range corresponding to the presence of the fullerene entity was also observed around 330 nm. A new weak broad band in the wavelength range of 750–1000 nm was found at higher concentrations of the dyad, as shown in Fig. 1b. Control experiments performed by recording the spectrum of MgP, and equimolar mixture of MgP and 2-phenylfulleropyrrolidine, revealed absence of this NIR band, suggesting that the interactions between MgP and C_{60} moieties of the dyad in the ground state are responsible of this new near IR absorption band. Similar spectral features have been reported in literature for closely associated porphyrin–fullerene systems.[26] The observed band-width (fwhm) for the Soret band of MgP*o*–C_{60} (6120 cm^{-1}) was found to be slightly larger than that of MgP (5660 cm^{-1}) in *o*-dichlorobenzene, which also suggests the existence of interactions between the MgP and C_{60} entities. In coordinating solvents (benzonitrile and DMF), the absorption peak of the Soret band exhibited red shifts of 3 nm compared to that in non-coordinating solvents (*o*-dichlorobenzene, anisole, and toluene), indicating that ligation of the coordinating solvents to the magnesium ion induces a considerable red shift (Fig. S2).†

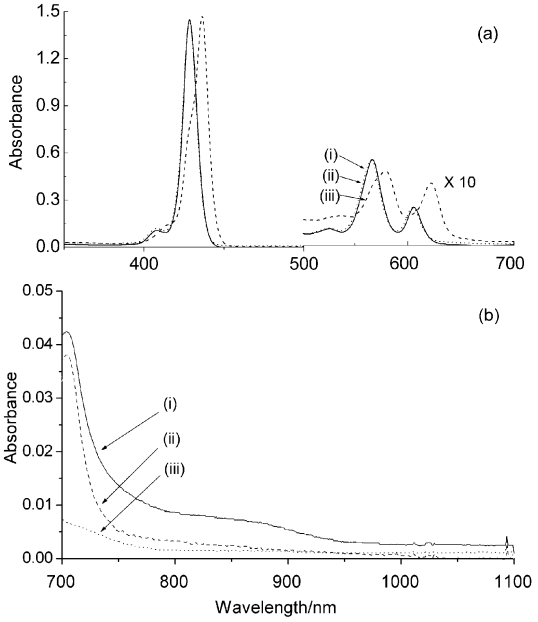

Fig. 1 (a) Absorption spectra of MgP*o*–C_{60} in (i) *o*-dichlorobenzene, (ii) benzonitrile, and (iii) pyridine in the visible region. The concentrations were held constant at 1.8 μM. (b) Near IR absorption spectra of (i) MgP*o*–C_{60}, (ii) equimolar MgP and 2-phenylfulleropyrrolidine, and (ii) MgP in *o*-dichlorobenzene.

In general, magnesium porphyrins can coordinate up to two axial ligands[27] unlike zinc porphyrins which bind to only one axial ligand. The spectrum of MgP*o*–C_{60} in the visible range in neat pyridine (Fig. 1a) showed red shifts characteristic of a bis-pyridine coordinated Mg porphyrin.[27] The pyridine binding constants for MgP*o*–C_{60} in *o*-dichlorobenzene were evaluated to be $K_1 = 2.2\ (\pm 0.2) \times 10^4\ M^{-1}$ and $K_2 = 1.1\ (\pm 0.13) \times 10^3\ M^{-1}$ (see supporting information for spectral details†). The magnitude of K_1 is comparable to that reported earlier for ZnP*o*–C_{60} in *o*-dichlorobenzene.[26] No clear evidence of the NIR band of MgP*o*–C_{60} in the presence of the pyridine was observed.

Ab initio B3LYP/3-21G(*) modeling of MP*o*–C_{60} (M = Mg and Zn) dyads

To gain insight into the molecular and electronic structure of the dyad, computational studies were performed using density functional methods (DFT) at the B3LYP/3-21G(*) level. The structures of the magnesium porphyrin–fullerene dyad in the presence and absence of pyridine (Fig. 2) were optimized to a stationary point on the Born–Oppenheimer potential energy surface. The key geometric parameters of the MP*o*–C_{60} (M = Zn and Mg) series of dyads are listed in Table 1. The highest occupied molecular orbital (HOMO) and lowest unoccupied molecular orbital (LUMO) are also shown in Fig. 2.

In the optimized structure, the MgP*o*–C_{60} dyad revealed closely spaced MgP and C_{60} entities (Fig. 2a). The center-to-center distance, R_{Ct-Ct}, between the MgP and fulleropyrrolidine was found to be 6.24 Å, while the edge-to-edge distance, R_{Ed-Ed}, was 2.82 Å. The R_{Ct-Ct} and R_{Ed-Ed} values were slightly longer than that calculated for ZnP*o*–C_{60} dyad being 6.19 and 2.65 Å, respectively.[26] Both the HOMO and LUMO were found to be π-type orbitals, and were localized on the porphyrin and fullerene entities, respectively (Fig. 2b and c). A small contribution of the HOMO (<2%) on the fullerene moiety was also observed.

The optimized structure of MgP*o*–C_{60} in the presence of two axially bound pyridine entities is shown in Fig. 2d. The R_{Ct-Ct} and R_{Ed-Ed} values between the MgP and fulleropyrrolidine were found to be 12.4 and 9.0 Å, respectively. A comparison

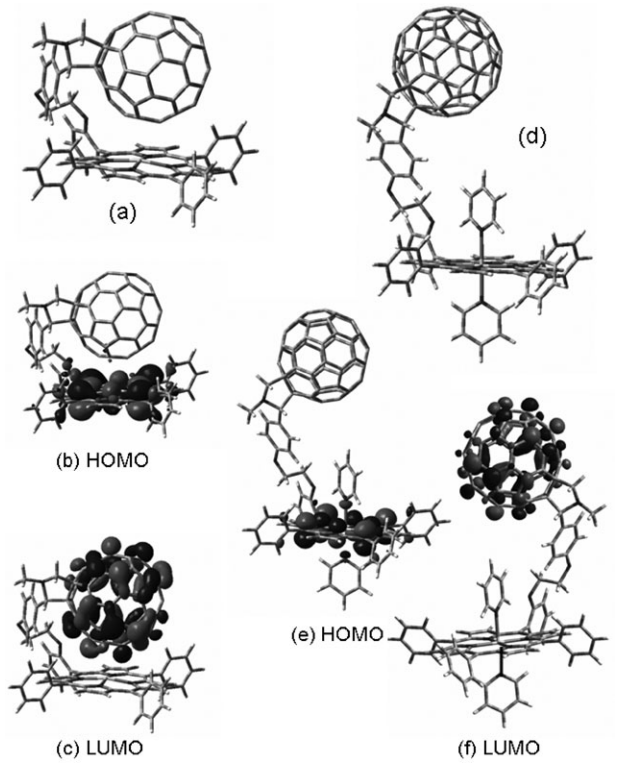

Fig. 2 *Ab initio* B3LYP/3-21G(*) optimized geometries of MgP*o*–C_{60} (a) in the absence and (d) in the presence of bis-pyridine ligands. Parts b, c, e and f show the HOMO and LUMO of the dyad under the conditions described in a and d.

between the porphyrin and C_{60} distances in $(Py)_2 \rightarrow$ MgP*o*–C_{60} and Py $\rightarrow$ ZnP*o*– C_{60} suggest *ca.* 6 Å increase for the former dyad and *ca.* 0.3 Å increase for the latter dyad as a result of pyridine coordination. These observations suggest substantial increase in the donor–acceptor distance upon bis-pyridine coordination of MgP*o*–C_{60}. However, it may be mentioned here that the distance calculated is the maximum possible distance and shorter donor–acceptor distances are possible at different local minima of the dyad. The calculated HOMO and LUMO of $(Py)_2 \rightarrow$ MgP*o*–C_{60} were also π-type orbitals whose coefficients were mainly located on the porphyrin and fullerene entities, respectively (Figs. 2e and f). Delocalization of the HOMO on the axially bound pyridine entities to a small extent was also observed.

Cyclic voltammetry studies and electron transfer driving forces

Electrochemical studies were performed to evaluate the redox potentials, which yielded information about electron–donor and electron–acceptor properties in the ground states. These

Table 1 B3LYP/3-21G(*) optimized geometric parameters of MP*o*–C_{60} (M = Mg and Zn) dyads

Compound	R_{Ct-Ct}, Å[a]	R_{Ed-Ed}, Å[b]
MgP*o*–C_{60}	6.24	2.82
Py $\rightarrow$ MgP*o*–C_{60}	6.85	3.62
$(Py)_2 \rightarrow$ MgP*o*–C_{60}	12.43	9.00
ZnP*o*–C_{60}[c]	6.19	2.65
Py $\rightarrow$ ZnP*o*–C_{60}[c]	6.58	3.09

[a] Distance between center of porphyrin to the center of fullerene sphere. [b] Distance between the closely located porphyrin π-system carbon, and fullerene sphere carbon. [c] Slight difference in the values from the earlier reported one (ref. 26*a*) is a result of better optimization starting from different starting geometries of the dyads.

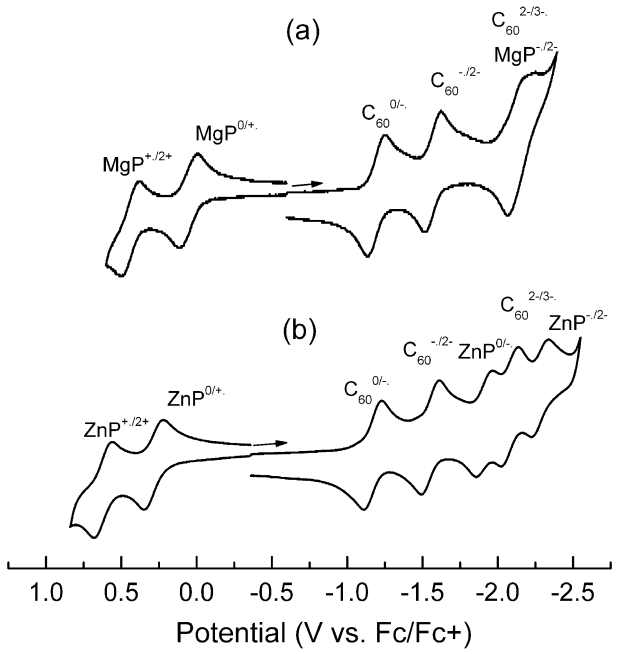

Fig. 3 Cyclic voltammograms of (a) MgP*o*–C_{60} and (b) ZnP*o*–C_{60} (*ca.* 0.05 mM) in *o*-dichlorobenzene [0.1 M $(n\text{-Bu})_4NClO_4$]. Scan rate = 100 mV s^{-1}. The site of electron transfer corresponding to each redox couple is indicated on the top of the voltammograms.

data also help to arrive at the energetics of the light-induced electron-transfer processes. Fig. 3 shows the cyclic voltammograms of MP*o*–C_{60} dyads (where M = Mg and Zn) in *o*-dichlorobenzene containing 0.1 M $(n\text{-Bu})_4NClO_4$ supporting electrolyte. Table 2 lists their redox potential values. Both of the porphyrins utilized here revealed two one-electron oxidations ($P^{0/\bullet+}$ and $P^{\bullet+/2+}$) as judged from their peak-to-peak separation, ΔE_{pp} values and the cathodic-to-anodic peak current ratios.[28] The magnitudes of the $E_{1/2}$ values were found to depend on the metal ion present in the porphyrin cavity which followed the order: MgP < ZnP, however, the corresponding redox potential values were close to that of the corresponding pristine metalloporphyrins. On the cathodic potential side, the first two one-electron reductions were found to involve fulleropyrrolidine ($C_{60}^{0/\bullet-}$ and $C_{60}^{\bullet-/2-}$), which were independent from MP. On the other hand, the subsequent reductions, depending upon M, involved either the porphyrin ($P^{0/\bullet-}$ and $P^{\bullet-/2-}$) or fullerene entity ($C_{60}^{2-/3\bullet-}$) as indicated against each redox couple in Fig. 3. A comparison between the first porphyrin ring oxidation potential of the dyads and the corresponding oxidation potential of pristine metal porphyrins in Table 2, revealed changes up to 30 mV, suggesting weak intramolecular interactions between the porphyrin and fullerene entities.

From these data, the driving forces for charge recombination ($-\Delta G_{CR}$) and charge separation ($-\Delta G_{CS}$) were calculated according to eqns. (1) and (2):[29]

$$-\Delta G_{CR} = E_{ox} - E_{red} - \Delta G_s \quad (1)$$

$$-\Delta G_{CS} = E_{0,0} - (-\Delta G_{CR}) \quad (2)$$

where E_{ox} is the first oxidation potential of the porphyrin ($P^{0/\bullet+}$), E_{red} is the first reduction potential of the fullerene ($C_{60}^{0/\bullet-}$), $\Delta E_{0,0}$ is the energy of the 0–0 transition between the lowest excited state and the ground state of the porphyrin and C_{60} as evaluated from the fluorescence peaks. These values are, respectively, 2.04 eV for ^{1}MgP*, 2.07 eV for ^{1}ZnP* and 1.75 eV for $^1C_{60}$*.[22] ΔG_S refers to the static energy, calculated by using the 'Dielectric continuum model' according to eqn. (3).[29]

$$\Delta G_S = e^2/(4\pi\varepsilon_0\varepsilon_S R_{Ct-Ct;}) \quad (3)$$

Table 2 Electrochemical half-wave redox potentials ($E_{1/2}$ *vs.* Fc/Fc^+) of porphyrin–fulleropyrrolidine dyads in the presence of 0.1 M $(n\text{-}Bu)_4NClO_4$ in benzonitrile (PhCN), *o*-dichlorobenzene (DCB), and pyridine (Py)

Compound	Solvent	$P^{\bullet+/2+}$/V	$P^{0/\bullet+}$/V	$C_{60}{}^{0/\bullet-}$ /V	$\Delta G_{CR}{}^{a}$ /eV	
MgTPP	DCB	0.46	0.07			[b]
MgP*o*–C_{60}	PhCN	0.51	0.20	−1.04	1.19	[c]
	DCB	0.43	0.06	−1.20	1.02	[c]
	Py-DCB[d]		0.18	−1.19	1.25	[c]
ZnTPP	DCB	0.62	0.28			[b]
ZnP*o*–C_{60}	PhCN	0.67	0.29	−1.04	1.23	[b]
	DCB	0.63	0.29	−1.17	1.22	[b]
	Py-DCB[d]		0.23	−1.17	1.23	[b]
2-Phenyl fullero-pyrrolidine				−1.14		[b]

[a] From eqns. (1) and (3). [b] From ref. 25 and 26*a*. [c] This work. [d] Obtained by addition of 50 eq. of pyridine to the DCB solution of porphyrins.

The symbols ε_0 and ε_s represent vacuum permittivity and dielectric constant of the solvent, respectively. The calculated $-\Delta G_{CR}$ values, corresponding to the energy of the radical ion-pairs, are summarized in Table 2. On the basis of the singlet emission and electrochemical data, the charge-separated state of MgP*o*–C_{60} lies below the first excited singlet states of MgP and C_{60} in toluene, anisole, dichlorobenzene, benzonitrile and DMF. Negative values of ΔG_{CS} were found to follow the order: ^{1}MgP*o**–C_{60} < ^{1}ZnP*o**–C_{60} in *o*-dichlorobenzene, indicating the expected higher exothermicity for electron transfer *via* the excited singlet states of the ^{1}MgP*o**–C_{60} compared to its zinc and free-base porphyrin analogs. However, by taking into consideration that the Weller model in toluene is likely to be oversimplified, it is possible to consider the energy of the charge-separated state of MgP*o*–C_{60} in toluene as slightly higher than that of $^3C_{60}$.

Steady-state emission studies

The excited state events of the MgP*o*–C_{60} were investigated, initially, by using steady-state fluorescence measurements in *o*-dichlorobenzene. Fig. 4 shows the fluorescence spectrum of MgP*o*–C_{60} along with the reference compound, MgTPP under the same solution concentrations, and when excited at the wavelength of the most intense visible band of MgP. Appreciable red shifts and decrease of the fluorescence intensities of MgTPP in benzonitrile and pyridine compared with those in *o*-dichlorobenzene are clear evidence of axial coordination of these solvents. The fluorescence quantum yields of ^{1}MgP*o*–C_{60} in *o*-dichlorobenzene, benzonitrile, and pyridine were found to be less than about 0.03 compared to that of pristine MgTPP, indicating efficient quenching of the magnesium porphyrin singlet excited state of the dyad in these solvents. The quenching process may involve energy and/or electron transfer pathways. To further understand the quenching mechanism in MgP*o*–C_{60} and to follow the kinetics of photoinduced processes, picosecond time-resolved emission and nanosecond transient absorption studies were performed in different solvents.

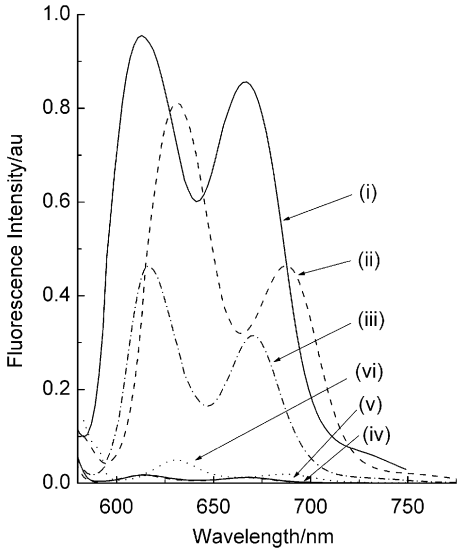

Fig. 4 Fluorescence spectra of magnesium tetraphenylporphyrin, MgP (curves i, ii and iii) and MgP*o*–C_{60} (curves iv, v, and vi) in *o*-dichlorobenzene (curves i and iv), benzonitrile (curves iii and vi), and pyridine (curves ii and v) (λ_{ex} = 565 nm in *o*-dichlorobenzene, 566 nm in benzonitrile and 579 nm in pyridine). The concentration of all of the species was held at 1.85 μM.

Time-resolved fluorescence studies

The time-resolved fluorescence spectra of the MgP*o*–C_{60} dyad are shown in Fig. 5; the spectra at 0.1 ns tracked those of the steady-state measurements in polar and nonpolar solvents, which are attributed to the ^{1}MgP* moiety of the MgP*o*–C_{60} dyad. In toluene, with the decrease in the transient fluorescence intensity of the ^{1}MgP* moiety, a new fluorescence peak appeared near 725 nm due to the $^1C_{60}$* moiety as shown in the spectrum recorded at the 0.5 ns time interval. This weak fluorescence corresponding to the $^1C_{60}$* moiety was also observed at the 0.5 ns time intervals in *o*-dichlorobenzene and anisole. The transient appearance of the fluorescence of the $^1C_{60}$* moiety in toluene, anisole and *o*-dichlorobenzene suggests the build-up of the $^1C_{60}$* moiety due to the energy transfer from the ^{1}MgP* moiety. However, to observe such fluorescence of the $^1C_{60}$* moiety, slower decay of the $^1C_{60}$*

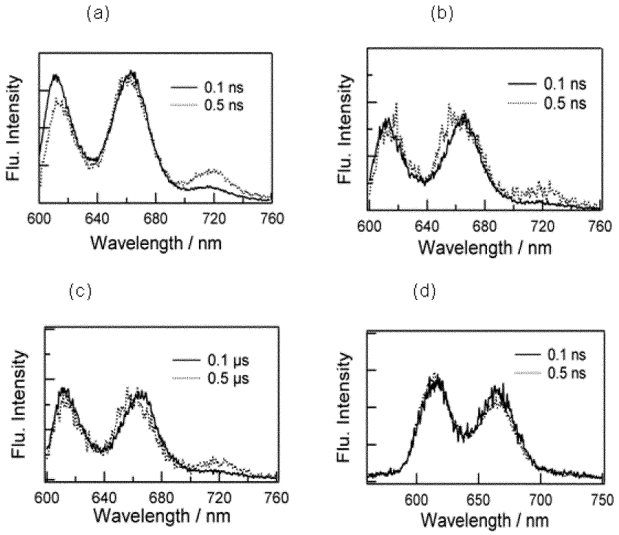

Fig. 5 Time-resolved fluorescence spectra of MgP*o*–C_{60}; (a) toluene, (b) anisole, (c) *o*-dichlorobenzene, and (d) benzonitrile.

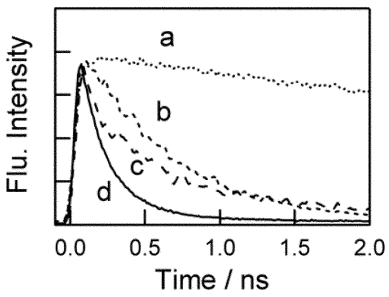

Fig. 6 Fluorescence decay profiles (a) MgP (600–700 nm) and (b) C_{60} (700–800 nm) and (c) MgP*o*–C_{60} (700–800 nm) and (d) MgP*o*–C_{60} (600–700 nm) dyad in an argon saturated *o*-dichlorobenzene (λ_{ex} = 400 nm). The concentration of all of the species was held at 0.05 mM.

moiety (from the subsequent photochemical reactions) may be a necessary factor. In a more polar solvent such as benzonitrile, the fluorescence enhancement of the $^1C_{60}$* moiety near 725 nm was not appreciable. This suggests two possibilities; one is absence of energy transfer from the ^{1}MgP* to C_{60} and another is occurrence of rapid charge separation from the $^1C_{60}$* moiety. Since the $^1C_{60}$* build-up revealed a systematic trend with the solvent polarity, the weak build-up of $^1C_{60}$* in more polar benzonitrile is attributed to occurrence of rapid charge separation from the fullerene singlet excited state.

The fluorescence decay-time profiles of the MgP moiety in MgP*o*–C_{60} dyad along with the reference compound, MgTPP in *o*-dichlorobenzene collected over the 600–680 nm spectral range (Fig. 6) indicated the occurrence of rapid fluorescence quenching of ^{1}MgP*o** in the dyad. From the monoexponential fluorescence decays, the lifetimes of the ^{1}MgP* moiety $(\tau_f^P)_{sample}$ of MgP*o*–C_{60} and reference $(\tau_f^P)_{ref}$ were evaluated as summarized in Table 3. From these $(\tau_f^P)_{sample}$ and $(\tau_f^P)_{ref}$ values, the quenching rate constants (k_q^P) and quantum yields (Φ_q^P) were evaluated using eqns. (4) and (5).

$$k_q^P = (1/\tau_f^P)_{sample} - (1/\tau_f^P)_{ref} \quad (4)$$

$$\Phi_q^P = [(1/\tau_f^P)_{sample} - (1/\tau_f^P)_{ref}]/(1/\tau_f^P)_{sample} \quad (5)$$

As listed in Table 3, the k_q^P and Φ_q^P values slightly increase with the decrease of the refractive index of the employed solvents, suggesting the occurrence of Förster-type energy-transfer *via* the ^{1}MgP* moiety.[30] In the case of DMF, large k_q^P and Φ_q^P values were obtained in spite of its low refractive index, suggesting a partial contribution of the charge-separation process *via* ^{1}MgP*.

The fluorescence lifetimes of the $^1C_{60}$* moiety were evaluated from the fluorescence decays in the 710–750 nm region. As shown in Fig. 6, a comparison of the time profile of the $^1C_{60}$* moiety of MgP*o*–C_{60} with that of pristine $^1C_{60}$* in *o*-dichlorobenzene revealed that the fluorescence decay rate of the former was faster than that of the latter. The fluorescence lifetimes of the $^1C_{60}$* moiety were in the range of 0.68 ns (in toluene), −0.41 ns (in DMF) by curve-fitting with single exponential decay. Since these lifetimes may be strongly affected by the rapid decay of the ^{1}MgP* moiety, we estimated the fluorescence lifetimes (τ_f^C) of the $^1C_{60}$* moiety after 0.5 ns as listed in Table 3. Since the τ_f^C values become short with increasing solvent polarity, the charge-separation process can be considered on combining the calculated negative ΔG_{CS} values. Thus, from these τ_f^C values, the charge-separation rate-constants (k_{CS}^C) and quantum-yields (Φ_{CS}^C) were evaluated according to eqns. (4) and (5) by replacing τ_f^C instead of τ_f^P. The k_{CS}^C values increased from 7.0×10^8 s^{-1} in toluene to 1.7×10^9 s^{-1} in DMF; the Φ_{CS}^C values increased from 0.47 to 0.69 for the MgP*o*–C_{60} dyad in these solvents, respectively.

From these results, we could explain the transient appearance of the fluorescence of the $^1C_{60}$* moiety at 720 nm at longer time scales in the time-resolved spectra. In polar solvents, since the k_{CS}^C values are almost the same as the k_q^P values, the transient fluorescence of the $^1C_{60}$* moiety was difficult to observe, although the k_q^P values are attributed to energy transfer. On the other hand, in less polar solvents where k_q^P ($\approx k_{EN}^P$) > k_{CS}^C, it was possible to observe the transient fluorescence of the $^1C_{60}$* moiety, as shown in Fig. 5. Even in nonpolar toluene, charge-separation *via* the $^1C_{60}$* moiety was anticipated to occur from the calculated negative ΔG_{CS} value and the observed rapid decay of the fluorescence of the $^1C_{60}$* moiety. Therefore, the expected initial rise of the fluorescence of the $^1C_{60}$* moiety[15c] due to energy-transfer from the ^{1}MgP* moiety was not observed.

The time-resolved fluorescence studies were also performed for the zinc porphyrin analog, ZnP*o*–C_{60} to verify the quenching mechanism. Earlier,[26] based on the free-energy calculations, time-resolved emission, and picosecond transient absorption spectral studies, we attributed the decay of ^{1}ZnP* moiety in ZnP*o*–C_{60} to charge separation. However, the present time-resolved fluorescence studies on ZnP*o*–C_{60} revealed the occurrence of transient fluorescence of the $^1C_{60}$* moiety upon excitation of ZnP in the dyad (see ESI).† These results suggest occurrence of energy transfer from ^{1}ZnP* to C_{60}, a result similar to that observed for the presently investigated, MgP*o*–C_{60} dyad. Subsequent charge separation from the $^1C_{60}$* moiety occurs after the energy transfer from the ^{1}ZnP* moiety. From the accelerated fluorescence decay of the $^1C_{60}$* moiety, both k_{CS}^C and Φ_{CS}^C values were newly evaluated, as listed in Table 3.

Table 3 Fluorescence lifetimes (τ_f), refractive index of the solvents (n), solvent polarity (ε), quenching rate-constants (k_q^P), quenching quantum-yields (Φ_q^P) *via* ^{1}MP*, charge-separation rate-constants (k_{CS}^C), charge-separation quantum-yields (Φ_{CS}^C) and free-energy of charge-separation (ΔG_{CS}^C) *via* $^1C_{60}$* for MP*o*–C_{60} in different organic solvents

MP*o*-C_{60}	Solvent	n	ε	τ_f^P/ns [a]	k_q^P/s^{-1}	Φ_q^P	τ_f^C/ns [a]	k_{CS}^C/s^{-1} [a]	Φ_{CS}^C	ΔG_{CS}^C/eV [b]
MgP*o*–C_{60}	DMF	1.45	35	0.26	3.7×10^9	0.97	0.41	1.7×10^9	0.69	0.58[c]
	PhCN	1.52	25	0.28	3.4×10^9	0.96	0.49	1.3×10^9	0.62	0.56[b]
	DCB	1.55	10	0.34	2.8×10^9	0.95	0.58	9.5×10^8	0.55	0.73[b]
	Anisole	1.51	4.5	0.28	3.4×10^9	0.96	0.58	9.5×10^8	0.55	0.42[c]
	Toluene	1.49	2.3	0.23	5.2×10^9	0.97	0.68	7.0×10^8	0.47	0.22[c]
ZnP*o*–C_{60}	DMF	1.45	35	0.27	3.2×10^9[d]	0.87	0.34	2.2×10^9[d]	0.74	0.53[c]
	PhCN	1.52	25	0.28	3.1×10^9[d]	0.87[d]	0.39[d]	1.8×10^9[d]	0.70[d]	0.52[b]
	DCB	1.55	10	0.30	2.8×10^9[d]	0.86[d]	0.45[d]	1.5×10^9[d]	0.67[d]	0.53[b]
	Toluene	1.49	2.3	0.24	3.7×10^9[d]	0.88[d]	0.64[d]	8.5×10^8[d]	0.54[d]	0.15[c]

[a] The τ_f for reference compounds; τ_f(MgP) = 8.3 ns, τ_f(ZnP) = 2.1 ns and τ_f(C_{60}) = 1.3 ns. [b] From eqns. (2) and (3). [c] $\Delta G_S = (e^2/(4\pi\varepsilon_0))[(1/(2R_+) + 1/(2R_-) - 1/R_{Ct-Ct})/\varepsilon_S - (1/(2R_+) + 1/(2R_-))/\varepsilon_R]$, where ε_R refers to dielectric constant for redox measurement; R_+ = 4.8 Å, R_- = 4.2 Å, R_{Ct-Ct} = 6.24 Å for MgP*o*–C_{60} and 6.19 Å for ZnP*o*–C_{60}. [d] Re-measured and analyzed in the present study.

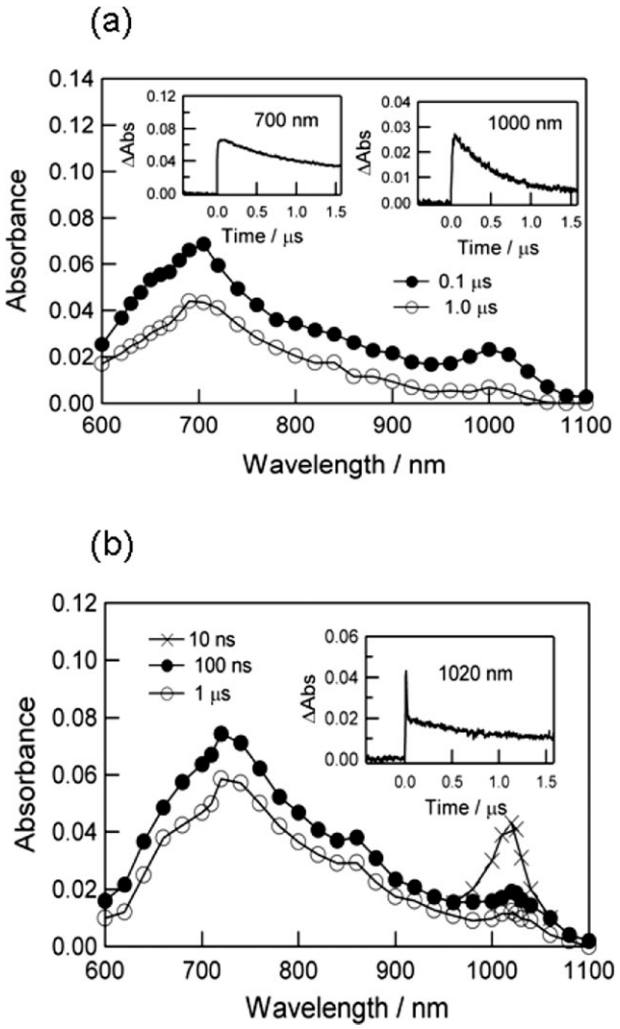

Fig. 7 Nanosecond transient absorption spectra of MgP*o*–C_{60} (0.05 mM) in argon saturated solution after the 532 nm-laser irradiation; (a) in *o*-dichlorobenzene, and (b) in toluene after the 532 nm-laser irradiation. Figure inset shows the time profiles of the transient bands at the indicated wavelengths.

Nanosecond transient absorption spectral investigations

Evidence for charge-separation and rate of charge recombination, k_{CR} values were obtained from nanosecond transient absorption spectral studies using 532 nm laser light. Fig. 7a shows the transient absorption spectra of the MgP*o*–C_{60} dyad in *o*-dichlorobenzene, which were almost the same as those in benzonitrile and DMF. Importantly, peaks corresponding to the formation of the fulleropyrrolidine anion radical, $C_{60}^{\bullet -}$ around 1020 nm[24] and MgP cation radical $MgP^{\bullet +}$ around 660 nm,[31] as evidence for the occurrence of photoinduced charge-separation in this dyad, were observed in addition to the absorption bands corresponding to the triplet state of the C_{60} entity ($^3C_{60}$*) at 700 nm with a shoulder at 870 nm.[32–33]

In *o*-dichlorobenzene, the decay of the $C_{60}^{\bullet -}$ entity around 1000 nm survived for more than 1.5 μs, which was shorter than the decay of the $^3C_{60}$* entity. Similar transient spectra were observed in polar solvents such as THF, benzonitrile, and DMF (see ESI).† From the decay of the 1020 nm band, the k_{CR} values of MgP*o*$^{\bullet +}$–$C_{60}^{\bullet -}$ in polar solvents were evaluated to be (1.9–3.3) $\times$ 10^6 s^{-1} as listed in Table 4. Using the k_{CR} values, the lifetimes of the radical ion-pair, τ_{RIP} ($=1/k_{CR}$) were evaluated as listed in Table 4. The τ_{RIP} value for MgP*o*–C_{60} in *o*-dichlorobenzene was found to be 510 ns and was longer than that of ZnP*o*–C_{60} (Table 4), suggesting that MgP*o*–C_{60} dyad is a better donor–acceptor system for applications related to photo-energy conversion.

Table 4 Charge-recombination rate-constants (k_{CR}) for MgP*o*–C_{60} in different organic solvents

MP*o*-C_{60}	Solvent	k_{CR}/s^{-1}	τ_{RIP}/ns	
MgP*o*–C_{60}	DMF	3.3×10^6	300	*a*
	PhCN	2.3×10^6	430	*a*
	THF	2.7×10^6	370	*a*
	DCB	1.9×10^6	510	*a*
	Py-DCB	1.8×10^6	550	*a*
	DNPy-DCB	1.7×10^6	580	*a*
	Anisole	2.3×10^6	440	*a*
	Toluene	1.8×10^8	<10	*a*
ZnP*o*–C_{60}	PhCN	1.8×10^6	560	*b*
	DCB	5.9×10^7	20	*b*
	Py-DCB	2.2×10^6	450	*b*

[a] This work. [b] From ref. 26*a*.

In toluene, on the other hand, a quick decay of the $C_{60}^{\bullet -}$ entity around 1020 nm was observed, indicating short lifetime of the $C_{60}^{\bullet -}$ entity, while the slow decay part at this wavelength was attributed to the time profiles of the tails of the triplet states of the MgP and C_{60} entities (Fig. 7b). The k_{CR} value calculated from the decay of the 1020 nm band was found to be 1.8×10^8 s^{-1}, as listed in Table 4. In anisole, a similar two-component decay was observed, giving k_{CR} values of 7.6×10^7 s^{-1} and 1.9×10^6 s^{-1}, respectively. The values of k_{CR} for MgP*o*$^{\bullet +}$–$C_{60}^{\bullet -}$ were found to vary from 2.8×10^6 s^{-1} in polar benzonitrile to 1.8×10^6 s^{-1} in less polar *o*-dichlorobenzene and anisole, suggesting the occurrence of charge-recombination in the inverted region of Marcus parabola.[8,14,16–18] However, the large k_{CR} value in toluene (and anisole) can not be explained by the Marcus theory.

In the case of ZnP*o*–C_{60}, addition of pyridine prolonged the τ_{RIP} of ZnP*o*$^{\bullet +}$–$C_{60}^{\bullet -}$ up to 450 ns, which is attributed to the delocalization of $ZnP^{\bullet +}$ to the coordinated pyridine.[26] Such a trend was also observed for the currently investigated MgP*o*–C_{60} dyad. That is, the τ_{RIP} value of MgP*o*$^{\bullet +}$–$C_{60}^{\bullet -}$ increased up to 550 ns upon addition of pyridine and up to 580 ns upon addition of dimethylaminopyridine (DNPy) to a *o*-dichlorobenzene solution containing MgP*o*–C_{60} (Table 4). These observations suggest occurrence of additional stabilization of the charge-separated states upon axial coordination of pyridine bases in metalloporphyrin–fullerene dyads. The observed longer lifetime of the radical ion-pairs in pyridine complexes could be ascribed to one or both of the following effects: (i) coordination of benzonitrile to the MgP which increases the center-to-center distance; and (ii) the declocalization of the π radical cation of MgP to the coordinated pyridine ligand.

Energy level diagram

Fig. 8 presents the energy level diagram for MgP*o*–C_{60}, in which the reported energy levels of the excited singlet and triplet states were employed.[16*c*] From the fast fluorescence decay of ^{1}MgP*, the energy transfer predominantly occurs from the porphyrin excited singlet state to the C_{60} moiety. After energy transfer, charge-separation occurred through the $^1C_{60}$* entity in polar and nonpolar solvents. In polar solvents including *o*-dichlorobenzene and anisole (Fig. 8a), the energy level of MgP*o*$^{\bullet +}$–$C_{60}^{\bullet -}$ was sufficiently lower than that of the $^1C_{60}$* entity, generating charge-stabilized radical ion-pair *via* the $^1C_{60}$* entity. The charge recombination of the radical ion-pair occurs to the ground state, because MgP*o*$^{\bullet +}$–$C_{60}^{\bullet -}$ was sufficiently higher than that of the $^3C_{60}$* entity. However, in toluene (Fig. 8b), it is likely that MgP*o*$^{\bullet +}$–$C_{60}^{\bullet -}$ decayed by charge recombination process to yield the $^3C_{60}$* entity, because the energy level of MgP*o*$^{\bullet +}$–$C_{60}^{\bullet -}$ is located slightly higher

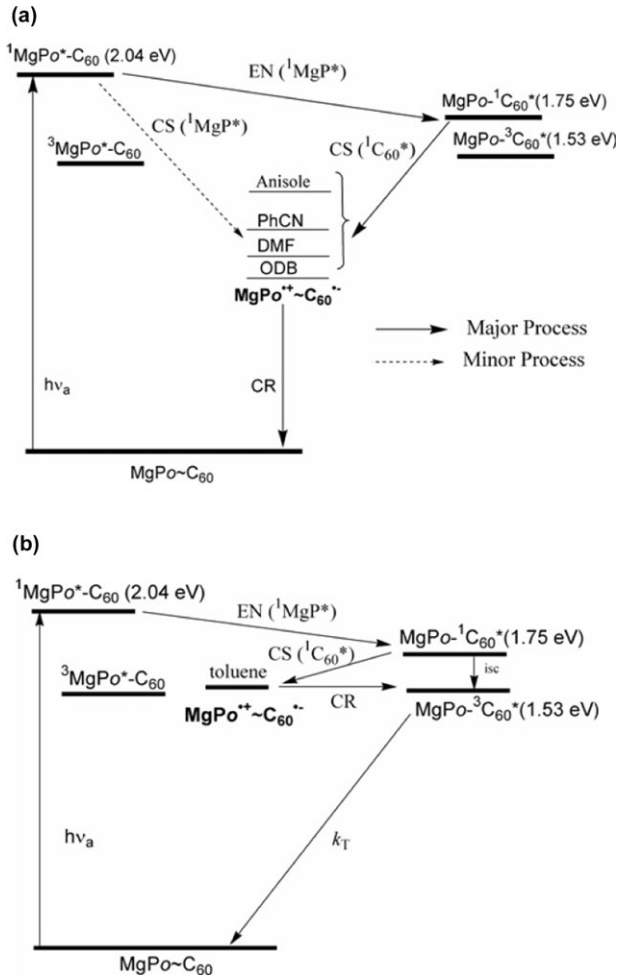

Fig. 8 Energy level diagrams showing the photochemical events of the MgP*o*–C_{60} dyad in (a) DMF, benzonitrile, *o*-dichlorobenzene and anisole, and (b) toluene.

than the energy level of the $^3C_{60}$*. This process might explain the short lifetime of the radical ion pair in toluene.

For ZnP*o*–C_{60}, a similar energy level diagram can be drawn, supporting the proposal that similar photoinduced processes to MgP*o*–C_{60} occur. The fast charge-recombination process of ZnP*o*–C_{60} in *o*-dichlorobenzene, however, resulted in short-lived radical ion-pairs. This may be due to the closely located energy levels of ZnP*o*$^{•+}$–$C_{60}^{•-}$ and $^1C_{60}$*, which would result in short-lived radical ion-pairs.

Comparison with intra- and intermolecularly interacting magnesium porphyrin–fullerene dyads

Recently, we reported light induced electron transfer in a self-assembled dyad involving magnesium tetraphenylporphyrin, MgTPP, with imidazole functionalized fullerene, C_{60}Im.[25] Additionally, electron transfer in intermolecular magnesium octaethylporphyrin and chlorophyll-*a*/−*b* with pristine C_{60} was also reported.[24] In the latter systems, the intermolecular electron transfer occurred either *via* the triplet states of MgTPP and chlorophylls or *via* the triplet state of C_{60}, depending on the excitation wavelength, giving solvated radical ions. On the other hand, in the coordinated supramolecular system (C_{60}Im → MgTPP), the charge-separation predominantly occurred within the supramolecular dyad *via* the initially excited ^{1}MgTPP*.[25] Since the thermodynamic properties are almost the same for both the self-assembled and covalently linked systems, the preferential energy transfer in MgP*o*–C_{60} can be attributed to the close proximity of the MgP moiety to the C_{60} sphere, which is advantageous for the Förster-type energy-transfer.[30]

Interestingly, the charge-recombination rate constant, k_{CR} for MgP*o*$^{•+}$–$C_{60}^{•-}$ is slower than that of C_{60}Im$^{•-}$ → MgTPP$^{•+}$ with a longer R_{Ct-Ct}. In the case of C_{60}Im$^{•-}$ → MgTPP$^{•+}$, the back electron transfer occurs *via* through-coordinated bonds, resulting in a faster rate. On the other hand, the charge-recombination in MgP*o*$^{•+}$–$C_{60}^{•-}$ may occur either through space or through covalent bonds *via* the ethylene oxide links; both mechanisms may decelerate the back electron transfer process compared with short through-coordination bond. It is worthwhile to note that the driving force dependence of the k_{CR} values is large, if the tunneling mechanism (through-space) is operating for the charge-recombination process in the inverted region of the Marcus parabola.[34] Our results showed that only a small decrease in the k_{CR} values was observed by changing the ΔG_{CR} values from anisole ($-\Delta G_{CR}$ = 1.62) to DMF ($-\Delta G_{CR}$ = 1.46). On the other hand, a larger difference for the k_{CR} values by a much smaller driving force difference has been reported previously for the linear covalently bonded ZnP$^{•+}$–$C_{60}^{•-}$,[16] where charge-recombination occurred *via* a through-bond mechanism. Therefore, the charge recombination mechanism for MgP*o*$^{•+}$–$C_{60}^{•-}$ may not involve the through-space tunneling mechanism.

Conclusion

The results of the present investigation demonstrate that magnesium porphyrins are suitable candidates for building covalently linked porphyrin–fullerene dyads for the study of light-induced energy- and electron-transfer processes. The easier oxidation and the longer fluorescence lifetime of MgP as compared to ZnP entity are some of the important features of MgP that have been effectively utilized in the construction and study of the present covalently linked, and the recently published self-assembled supramolecular dyads.[25] As a result, efficient photo-induced energy/electron transfer and relatively long-lived charge separated states have been achieved in the majority of the studied solvents.

Experimental

Chemicals

Buckminsterfullerene, C_{60} (+99.95%) was from SES Research, (Houston, TX). The solvents in sure seal bottles and chemicals utilized in the synthesis were from Aldrich Chemicals (Milwaukee, WI). Tetra-*n*-butylammonium perchlorate, $(n\text{-Bu})_4NClO_4$ was from Fluka Chemicals. The syntheses and purification of MP*o*–C_{60} (M = 2H and Zn) were carried out according to our previous procedure.[26]

meso-Tetraphenylporphyrinatomagnesium(II), MgP

This was prepared according to a general procedure developed by Lindsey and Woodford for Mg porphyrin synthesis.[35]To a 100 mg of free-base tetraphenylporphyrin, H_2P taken in 30 mL of CH_2Cl_2, 20 eq. of triethylamine and 10 eq. of $MgBr_2 \cdot O(Et)_2$ were added. The mixture was stirred for 30 min at room temperature. The course of the metallation reaction was monitored by absorption spectroscopy to the disappearance of the 515 nm band of free-base porphyrin. The mixture was washed with 5% $NaHCO_3$, dried over anhydrous Na_2SO_4, and purified on a silica gel column using toluene and chloroform as eluent. Yield = 85%. ^{1}H NMR (400 MHz, [D_1]$CHCl_3$, 25 °C, TMS): δ/ppm: 8.89 (s, 8H, β-pyrrole-H), 8.23 (d, 8H, *ortho*-phenyl-H), 7.74 (m, 12H, *meta*- and *para*-phenyl-H). ESI mass in CH_2Cl_2: calcd. 636.3, found 637.5. ESI mass in CH_2Cl_2: calcd. 637.03, found 636. UV-Vis (*o*-dichlorobenzene) λ_{max}: 428.5, 565, and 604.5 nm.

MgP*o*–C_{60}

H_2P*o*–C_{60} (80 mg) was taken in 30 mL of CH_2Cl_2 and 20 eq. of triethylamine and 10 eq. of $MgBr_2 \cdot O(Et)_2$ were added. The mixture was stirred for 30 min at room temperature. The course of the reaction was monitored by absorption spectroscopy. The mixture was diluted with CH_2Cl_2 and washed with 5% $NaHCO_3$, and dried over anhydrous Na_2SO_4. The desired compound was obtained after purification on a silica gel (9 : 1 toluene: $CHCl_3$). Yield = *ca.* 78%. It may be mentioned here that metallation of H_2P*o*–C_{60} by the conventional reaction involving magnesium acetate in $CHCl_3$:CH_3OH (1 : 1) mixture did not yield the desired compound. ^{1}H NMR (400 MHz, [D_1]$CHCl_3$, 25 °C, TMS): δ/ ppm: 8.8 (m, 8H, β-pyrrole-H), 8.2 (m, 6H, *ortho*-phenyl-H), 7.7 (m, 9H, *meta*- and *para*-phenyl-H), 7.24–7.05 (m, 4H, substituted phenyl-H), 6.91 (broad s, 2H, phenyl H), 5.91 (s, 2H, phenyl-H), 4.05, 3.41 (t,t, 2H,2H, CH_2-CH_2), 4.75, 3.97 (d,d, 2H, pyrrolidine-H), 4.5 (s, 1H, pyrrolidine-H), 2.15 (s, 3H, pyrrolidine N-CH_3). ESI mass in CH_2Cl_2: calcd. 1548.4, found 1549.5. UV-Vis (*o*-dichlorobenzene) λ_{max}: 429, 565.5, and 604.5 nm.

Instrumentation

The UV-visible spectral measurements were carried out with a Shimadzu Model 1600 UV-visible spectrophotometer. The fluorescence emission was monitored by using a Spex Fluorolog-tau spectrometer. The ^{1}H NMR studies were carried out on a Varian 400 MHz spectrometer. Tetramethylsilane (TMS) was used as an internal standard. Cyclic voltammograms were recorded on a EG&G Model 263A potentiostat using a three electrode system. A platinum button or glassy carbon electrode was used as the working electrode. A platinum wire served as the counter electrode and an Ag/AgCl was used as the reference electrode. Ferrocene/ferrocenium redox couple was used as an internal standard. All the solutions were purged prior to the electrochemical and spectral measurements using argon gas. The computational calculations were performed by *ab initio* B3LYP/3-21G(*) methods with GAUSSIAN 03[36] software package on high speed computers. The images of the frontier orbitals were generated from Gauss View-03 software. The ESI-mass spectral analyses of the newly synthesized compounds were performed by using a Fennigan LCQ-Deca mass spectrometer. For this, the compounds (about 0.1 mM) were prepared in CH_2Cl_2, freshly distilled over calcium hydride.

Time-resolved emission and transient absorption measurements

The picosecond time-resolved fluorescence spectra were measured using an argon-ion pumped Ti:sapphire laser (Tsunami) and a streak scope (Hamamatsu Photonics). Nanosecond transient absorption spectra in the near-IR region were measured by means of laser-flash photolysis; 532 nm light from a Nd:YAG laser was used as an exciting source and a Ge-avalanche-photodiode module was used for detecting the monitoring light from a pulsed Xe-lamp as described in our previous report.[37]

Acknowledgements

We are thankful to Prof. David. I. Schuster for helpful suggestions. The authors are thankful to the donors of the Petroleum Research Fund administered by the American Chemical Society, National Science Foundation, Grant-in-Aid for the COE project, Giant Molecules and Complex Systems, 2002 (to MEK), and for Scientific Research on Priority Area (417) from the Ministry of Education, Science, Sport and Culture of Japan (to OI add YA) for support of this work. P.A.K. is thankful to NSF for a RSEC fellowship.

References

1 (*a*) R. A. Marcus and N. Sutin, *Biochim. Biophys. Acta*, 1985, **811**, 265; (*b*) R. A. Marcus, *Angew. Chem.*, 1993, **105**, 1167; (*c*) R. A. Marcus, *Angew. Chem., Int. Ed. Engl.*, 1993, **32**, 1111; (*d*) M. Bixon and J. Jortner, *Adv. Chem. Phys.*, 1999, **106**, 35.

2 (*a*) J. R. Winkler and H. B. Gray, *Chem. Rev.*, 1992, **92**, 369; (*b*) C. Kirmaier and D. Holton, in *The Photosynthetic Reaction Center*, ed. J. Deisenhofer and J. R. Norris, Academic Press, San Diego, 1993, vol. II, pp. 49–70.

3 (*a*) G. McLendon and R. Hake, *Chem. Rev.*, 1992, **92**, 481; (*b*) I. R. Gould and S. Farid, *Acc. Chem. Res.*, 1996, **29**, 522; (*c*) F. D. Lewis, R. L. Letsinger and M. R. Wasielewski, *Acc. Chem. Res.*, 2001, **34**, 159.

4 (*a*) J. R. Miller, L. T. Calcaterra and G. L. Closs, *J. Am. Chem. Soc.*, 1984, **106**, 3047; (*b*) G. L. Closs and J. R. Miller, *Science*, 1988, **240**, 440; (*c*) J. S. Connolly and J. R. Bolton, in *Photoinduced Electron Transfer*, ed. M. A. Fox and M. Chanon, Elsevier, Amsterdam, 1988, Part D, pp. 303–393.

5 (*a*) M. R. Wasielewski, *Chem. Rev.*, 1992, **92**, 435; (*b*) H. Kurreck and M. Huber, *Angew. Chem.*, 1995, **107**, 929; (*c*) H. Kurreck and M. Huber, *Angew. Chem., Int. Ed. Engl.*, 1995, **34**, 849; (*d*) D. Gust, T. A. Moore and A. L. Moore, *Acc. Chem. Res.*, 2001, **34**, 40.

6 (*a*) A. Harriman and J.-P. Sauvage, *Chem. Soc. Rev.*, 1996, **26**, 41; (*b*) M.-J. Blanco, M. C. Jiménez, J.-C. Chambron, V. Heitz, M. Linke and J.-P. Sauvage, *Chem. Soc. Rev.*, 1999, **28**, 293; (*c*) V. Balzani, A. Juris, M. Venturi, S. Campagna and S. Serroni, *Chem. Rev.*, 1996, **96**, 759; (*d*) *Electron Transfer in Chemistry*, ed. V. Balzani, Wiley-VCH, Weinheim, 2001.

7 (*a*) M. N. Paddon-Row, *Acc. Chem. Res.*, 1994, **27**, 18; (*b*) J. W. Verhoeven, *Adv. Chem. Phys.*, 1999, **106**, 603; (*c*) K. Maruyama, A. Osuka and N. Mataga, *Pure Appl. Chem.*, 1994, **66**, 867; (*d*) A. Osuka, N. Mataga and T. Okada, *Pure Appl. Chem.*, 1997, **69**, 797.

8 (*a*) H. Imahori and Y. Sakata, *Eur. J. Org. Chem.*, 1999, 2445; (*b*) D. M. Guldi, *Chem. Commun.*, 2000, 321; (*c*) M. E. El-Khouly, O. Ito, P. M. Smith and F. D'Souza, *J. Photochem. Photobiol., C*, 2004, **5**, 79.

9 (*a*) J. S. Sessler, B. Wang, S. L. Springs and C. T. Brown, in *Comprehensive Supramolecular Chemistry*, ed. J. L. Atwood, J. E. D. Davies, D. D. MacNicol and F. Vögtle, Pergamon, 1996, ch. 9; (*b*) T. Hayashi and H. Ogoshi, *Chem. Soc. Rev.*, 1997, **26**, 355; (*c*) M. W. Ward, *Chem. Soc. Rev.*, 1997, **26**, 365.

10 (*a*) *Introduction of Molecular Electronics*, ed. M. C. Petty, M. R. Bryce and D.Bloor, Oxford University Press, New York, 1995; (*b*) *Molecular Switches*, ed. B. L. Feringa, Wiley-VCH GmbH, Weinheim, 2001.

11 (*a*) H. W. Kroto, J. R. Heath, S. C. O'Brien, R. F. Curl and R. E. Smalley, *Nature*, 1985, **318**, 162; (*b*) W. Kratschmer, L. D. Lamb, F. Fostiropoulos and D. R. Huffman, *Nature*, 1990, **347**, 345; (*c*) *Fullerene and Related Structures*, ed., A. Hirsch, Springer, Berlin, vol. 199, p. 1999.

12 *The Porphyrin Handbook*, ed. K. M. Kadish, K. M. Smith and R. Guilard, Academic Press, Burlington, MA, 2000, vol. 1–10.

13 (*a*) P. M. Allemand, A. Koch, F. Wudl, Y. Rubin, F. Diederich, M. M. Alvarez, S. J. Anz and R. L. Whetten, *J. Am. Chem. Soc.*, 1991, **113**, 1050; (*b*) Q. Xie, E. Perez-Cordero and L. Echegoyen, *J. Am. Chem. Soc.*, 1992, **114**, 3978; (*c*) B. S. Sherigara, W. Kutner and F. D'Souza, *Electroanalysis*, 2003, **15**, 753.

14 (*a*) N. Martín, L. Sánchez, B. Illescas and I. Pérez, *Chem. Rev.*, 1998, **98**, 2527; (*b*) M. Prato, *J. Mater. Chem.*, 1997, **7**, 1097; (*c*) F. Diederich and M. Gómez-López, *Chem. Soc. Rev.*, 1999, **28**, 263.

15 (*a*) H. Imahori, K. Hagiwara, T. Akiyama, M. Aoki, S. Taniguchi, T. Okada, M. Shirakawa and Y. Sakata, *Chem. Phys. Lett.*, 1996, **263**, 545; (*b*) D. M. Guldi and K.-D. Asmus, *J. Am. Chem. Soc.*, 1997, **119**, 5744; (*c*) H. Imahori, M. E. El-Khouly, M. Fujitsuka, O. Ito, Y. Sakata and S. Fukuzumi, *J. Phys. Chem. A*, 2001, **105**, 325; (*d*) D. I. Schuster, P. Cheng, P. D. Jarowski, D. M. Guldi, C. Luo, L. Echegoyen, S. Pyo, A. R. Holzwarth, S. E. Braslavsky, R. M. Williams and G. Klihm, *J. Am. Chem. Soc.*, 2004, **126**, 7257.

16 (*a*) C. Luo, D. M. Guldi, H. Imahori, K. Tamaki and Y. Sakata, *J. Am. Chem. Soc.*, 2000, **122**, 6535; (*b*) H. Imahori, D. M. Guldi, K. Tamaki, Y. Yoshida, C. Luo, Y. Sakata and S. Fukuzumi, *J. Am. Chem. Soc.*, 2001, **123**, 6617; (*c*) H. Imahori, K. Tamaki, Y. Araki, Y. Sekiguchi, O. Ito, Y. Sakata and S. Fukuzumi, *J. Am. Chem. Soc.*, 2002, **124**, 5165; (*d*) P. A. Liddell, G. Kodis, A. L. Moore, T. A. Moore and D. Gust, *J. Am. Chem. Soc.*, 2002, **124**, 7668; (*e*) N. Watanabe, N. Kihara, Y. Furusho, T. Takata,

Y. Araki and O. Ito, *Angew. Chem.*, 2003, **115**, 705; (*f*) N. Watanabe, N. Kihara, Y. Furusho, T. Takata, Y. Araki and O. Ito, *Angew. Chem. Int. Ed.*, 2003, **42**, 681; (*g*) K. Ohkubo, H. Kotani, J. Shao, Z. Ou, K. M. Kadish, G. Li, R. K. Pandey, M. Fujitsuka, O. Ito, H. Imahori and S. Fukuzumi, *Angew. Chem.*, 2004, **116**, 871; (*h*) K. Ohkubo, H. Kotani, J. Shao, Z. Ou, K. M. Kadish, G. Li, R. K. Pandey, M. Fujitsuka, O. Ito, H. Imahori and S. Fukuzumi, *Angew. Chem. Int. Ed.*, 2004, **43**, 853; (*i*) V. Chukharev, N. V. Tkachenko, A. Efimov, D. M. Guldi, A. Hirsh, M. Scheloske and H. Lemmetyinen, *J. Phys. Chem. B*, 2004, **108**, 16377.

17 (*a*) F. D'Souza, G. R. Deviprasad, M. E. Zandler, M. E. El-Khouly, M. Fujitsuka and O. Ito, *J. Phys. Chem. B*, 2002, **106**, 4952; (*b*) M. E. El-Khouly, S. Gadde, G. R. Deviprasad, M. Fujitsuka, O. Ito and F. D'Souza, *J. Porphyrins Phthalocyanines.*, 2003, **7**, 1; (*c*) F. D'Souza, G. R. Deviprasad, M. E. Zandler, M. E. El-Khouly, M. Fujitsuka and O. Ito, *J. Phys. Chem. A*, 2003, **107**, 4801; (*d*) F. D'Souza, P. M. Smith, M. E. Zandler, A. L. McCarty, M. Itou, Y. Araki and O. Ito, *J. Am. Chem. Soc.*, 2004, **126**, 7898; (*e*) F. D'Souza, P. M. Smith, S. Gadde, A. L. McCarty, M. J. Kullman, M. E. Zandler, M. Itou, Y. Araki and O. Ito, *J. Phys. Chem. B*, 2004, **108**, 11333; (*f*) F. D'Souza, M. E. El-Khouly, S. Gadde, M. E. Zandler, A. L. McCarty, Y. Araki and O. Ito, *Tetrahedron*, 2005, in press.

18 (*a*) K. Li, D. I. Schuster, D. M. Guldi, M. A. Herranz and L. Echegoyen, *J. Am. Chem. Soc.*, 2004, **126**, 3388; (*b*) D. M. Guldi, H. Imahori, K. Tamaki, Y. Kashiwagi, H. Yamada, Y. Sakata and S. Fukuzumi, *J. Phys. Chem. A*, 2004, **108**, 541; (*c*) P. A. Liddell, G. Kodis, J. Andreasson, G. L. De la, S. Bandyopadhyay, R. H. Mitchell, T. A. Moore, A. L. Moore and D. Gust, *J. Am. Chem. Soc.*, 2004, **126**, 4803.

19 (*a*) N. N. Greenwood and A. Earnshaw, *Chemistry of the Elements*, Pergamon, Oxford, 1984; (*b*) F. Li, S. Gentemann, W. A. Kalsbeck, J. Seth, J. S. Lindsey, D. Holten and D. F. Bocian, *J. Mater. Chem.*, 1997, **7**, 1245.

20 (*a*) G. D. Dorough, J. R. Miller and F. M. Huennekens, *J. Am. Chem. Soc.*, 1951, **73**, 4315; (*b*) J. B. Allison and R. S. Becker, *J. Chem. Phys.*, 1960, **32**, 1410.

21 K. M. Kadish, E. Van Caemelbecke and G. Royal, in *The Porphyrin Handbook*, ed. K. M. Kadish, K. M. Smith and R. Guilard, Academic Press, New York, 2000, vol 8, ch. 55, pp. 1–114.

22 (*a*) J. M. Zaleski, C. K. Chang, G. E. Leroi, R. I. Cukier and D. G. Nocera, *J. Am. Chem. Soc.*, 1992, **114**, 3564; (*b*) K. Wynne, S. J. LeCours, C. Galli, M. J. Therien and R. M. Hochstrasser, *J. Am. Chem. Soc.*, 1995, **117**, 3749; (*c*) J. Li, J. R. Diers, J. Seth, S. I. Yang, D. F. Bocian, D. Holten and J. S. Lindsey, *J. Org. Chem.*, 1999, **64**, 9090; (*d*) M. J. Natan and B. M. Hoffman, *J. Am. Chem. Soc.*, 1989, **111**, 6468; (*e*) P. Hascoat, S. I. Yang, R. K. Lammi, J. Alley, D. F. Bocian, J. S. Lindsey and D. Holten, *Inorg. Chem.*, 1999, **38**, 4849.

23 (*a*) S. I. Yang, R. K. Lammi, S. Prathapan, M. A. Miller, J. Seth, J. R. Diers, D. F. Bocian, J. S. Lindsey and D. Holten, *J. Mater. Chem.*, 2001, **11**, 2420; (*b*) A. Ambroise, R. W. Wagner, P. D. Rao, J. A. Riggs, P. Hascoat, J. R. Diers, J. Seth, R. K. Lammi, D. F. Bocian, D. Holten and J. S. Lindsey, *J. Mater. Chem.*, 2001, **13**, 1023.

24 (*a*) M. E. El-Khouly, Y. Araki, M. Fujitsuka, A. Watanabe and O. Ito, *Photochem. Photobiol.*, 2001, **74**, 22; (*b*) M. E. El-Khouly, Y. Araki, M. Fujitsuka and O. Ito, *Phys. Chem. Chem. Phys.*, 2002, **4**, 3322.

25 F. D'Souza, M. E. El-Khouly, S. Gadde, A. L. McCarty, P. A. Karr, M. E. Zandler, Y. Araki and O. Ito, *J. Phys. Chem. B*, 2005, **109**, 10107.

26 (*a*) F. D'Souza, S. Gadde, M. E. Zandler, A. Klyov, M. E. El-Khouly, M. Fujitsuka and O. Ito, *J. Phys. Chem. A*, 2002, **106**, 12393; (*b*) D. M. Guldi, C. Luo, M. Prato, A. Troisi, F. Zerbetto, M. Scheloske, E. Dietel, W. Bauer and A. Hirsch, *J. Am. Chem. Soc.*, 2001, **123**, 9166; (*c*) N. Armaroli, G. Marconi, L. Echegoyen, J.-P. Bourgeois and F. Diederich, *Chem. Eur. J.*, 2000, **6**, 1629; (*d*) F. D'Souza, R. Chitta, S. Gadde, M. E. Zandler, A. L. McCarty, A. S. D. Sandanayaka, Y. Araki and O. Ito, *Chem. Eur. J.*, 2005, **11**, 4416.

27 (*a*) J. R. Miller and G. D. Dorough, *J. Am. Chem. Soc.*, 1952, **74**, 3977; (*b*) K. M. Kadish and L. R. Shiue, *Inorg. Chem.*, 1982, **21**, 1112.

28 *Electrochemical Methods: Fundamentals and Applications*, A. J. Bard and L. R. Faulkner, John Wiley, New York, 2nd edn., 2001.

29 (*a*) D. Rehm and A. Weller, *Isr. J. Chem.*, 1970, **7**, 259; (*b*) N. Mataga, H. Miyasaka, in *Electron Transfer*, ed. J. Jortner and M. Bixon, John Wiley & Sons, New York, 1999, Part 2, pp. 431–496.

30 (*a*) T. Förster, *Naturwissenschaften*, 1946, **33**, 166–175; (*b*) T. Förster, *Ann. Phys.*, 1948, **2**, 55.

31 (*a*) A. Harriman, P. Neta and M.-C. Richoux, *J. Phys. Chem.*, 1986, **90**, 3444; (*b*) A. G. Skillman, J. R. Collins and G. H. Loew, *J. Am. Chem. Soc.*, 1992, **114**, 9538.

32 T. Nojiri, A. Watanabe and O. Ito, *J. Phys. Chem. A*, 1998, **102**, 5215.

33 (*a*) H. N. Ghosh, H. Pal, A. V. Sapre and J. P. Mittal, *J. Am. Chem. Soc.*, 1993, **115**, 11722; (*b*) M. Fujitsuka, O. Ito, T. Yamashiro, Y. Aso and T. Otsubo, *J. Phys. Chem. A*, 2000, **104**, 4876.

34 N. Liang, J. R. Miller and G. L. Closs, *J. Am. Chem. Soc.*, 1990, **112**, 5454.

35 J. S. Lindsey and J. N. Woodford, *Inorg. Chem.*, 1995, **34**, 1063.

36 *GAUSSIAN 03, (Revision B-04)*, Gaussian, Inc., Pittsburgh PA, 2003.

37 (*a*) K. Matsumoto, M. Fujitsuka, T. Sato, S. Onodera and O. Ito, *J. Phys. Chem. B*, 2000, **104**, 11632; (*b*) S. Komamine, M. Fujitsuka, O. Ito, K. Morikawa, T. Miyata and T. Ohno, *J. Phys. Chem. A*, 2000, **104**, 11497; (*c*) M. Yamazaki, Y. Araki, M. Fujitsuka and O. Ito, *J. Phys. Chem. A*, 2001, **105**, 8615.